

Force-Controlled Tensile Test of Collagen Fibril by Using 2-DOF Control System With Modeling Error Compensation

NAOKI MOTOI ^{1,2} (Member, IEEE), MATHIS NALBACH³, SHINGO ITO ^{2,4}, PHILIPP J. THURNER³,
AND GEORG SCHITTER ² (Senior Member, IEEE)

¹Graduate School of Maritime Sciences, Kobe University, Kobe 658-0022, Japan

²Automation and Control Institute, Vienna University of Technology, A-1040 Vienna, Austria

³Institute of Lightweight Design and Structural Biomechanics, Vienna University of Technology, A-1040 Vienna, Austria

⁴Department of Mechanical and System Engineering, University of Fukui, Fukui 910-8507, Japan

CORRESPONDING AUTHOR: NAOKI MOTOI (e-mail: motoi@maritime.kobe-u.ac.jp)

This work was supported in part by the Mitutoyo Association for Science and Technology and in part by the International Affairs Special Funding from the Graduate School of Maritime Sciences, Kobe University.

ABSTRACT Collagen is a major structural protein in the human body. It not only provides connective tissues such as ligaments and tendons with toughness and strength but it also constitutes the biomechanical scaffold for cell attachment in the extracellular matrix. Collagen molecules aggregate to form collagen fibrils, which are fibers with a diameter of 10 nm to 500 nm and a length of up to a centimeter. Tensile tests on individual collagen fibrils reveal a strongly non-linear stress-response to deformation with the tensile modulus reaching the gigapascal range. But not only that, collagen fibrils have been found to be viscoelastic which means collagen fibrils have both elastic and viscous characteristics. However, direct measurement of viscoelastic material properties in tension is only possible with force-controlled tensile tests, which can not be conducted with state-of-the-art methods. In this paper, we report the first force-controlled tensile tests of individual collagen fibrils. To account for the non-linear material characteristics, high responsiveness in the force control and robustness about a property change of the collagen fibril are needed. Therefore, a two-degrees-of-freedom (2-DOF) controller is applied for force control with high responsiveness. The 2-DOF controller is composed of feedforward (FF) and feedback (FB) controllers. In addition, a modeling error compensation is implemented for robustness. The modeling error is calculated from the difference between the actual force response measured by the sensor and the ideal force response calculated from the plant model. The validity of the proposed control method is confirmed from simulation and experimental results.

INDEX TERMS Force control, motion control, piezoelectric actuator, precision engineering, biomechanics.

I. INTRODUCTION

Precise motion control technology has been widely used in the industry, medical, and biological fields. As examples of the industry field, there have been various mechatronics products such as storage devices [1], [2], industrial machines [3], [4], and microscopes [5], [6]. In addition, nanomanipulation has been developed by applying microscope technology. Microscopes such as the scanning probe microscope (SPM) [7][8] and atomic force microscope (AFM) [9], [10] perform high-precision measurements by bringing the probe into

contact with the sample surface. By diverting this technology, nanomanipulation is realized.

For nanomanipulation, piezoelectric actuators have been widely used. Seki *et al.* presented the robust vibration suppression method by using the dual controller design in the piezo-actuated stage system [11]. Nguyen *et al.* combined the conventional feedback and adaptive feedforward methods for the precise piezo-actuated positioning systems [12]. Chen *et al.* developed the dynamic hysteresis model of the piezoelectric actuator and compensated the nonlinear

characteristics [13]. Researches on nanomanipulation using piezo actuators have also been reported. Shen *et al.* developed the method for single cell stiffness measurement based on a nano-needle and nanomanipulation [14]. Yang *et al.* reported the pile-up structure based nanopositioning mechanism driven by the piezoelectric actuator [15]. Mekid developed the integrated and numerically controlled instrument for nanomanipulation, imaging, and in-process inspection [16]. Yuan *et al.* developed the AFM tip position control for effective nanomanipulation [17].

To our best knowledge, this work aims to realize the first force-controlled tensile tests of individual collagen fibrils and other nano- and microfibers. This enables direct measurement of viscoelastic material properties, which is not possible with state-of-the-art methods. Collagen is the most abundant protein in human bodies and one of the few proteins that bears tensile load. It provides a majority of tissues with their mechanical properties, from tendons, ligaments, and bones to artery walls and the cornea of an eye [18]. At the nanoscale, collagen molecules aggregate to form collagen fibrils, which are nanoscale fibers with diameters in the range between 10 nm and 500 nm. The length of collagen fibrils can reach up to a centimeter. Collagen fibrils can easily be recognized by their periodically structured surface, commonly known as D-banding, as observed by AFM imaging or electron microscopy [18], [19]. Besides providing tissues passive mechanical function, collagen fibrils are the main constituent of the extra-cellular matrix (ECM). Collagens, therefore, play a crucial role in cell mechanotransduction [20]. There is increasing evidence, that ECM viscoelasticity is a major determinant of cell differentiation and proliferation. However, viscoelastic material parameters of individual collagen fibrils are currently unknown. In the course of diseases, such as diabetes and fibrosis, or during normal aging the mechanical properties of collagen fibril may change and negatively influence mechanotransduction and mechanobiology [21]–[23]. Currently, there is no method described in the literature that allows for true force-controlled tensile tests of collagen fibrils. Despite this, significant effort has been done in conducting monotonic but not well controlled tensile tests of single collagen fibrils. For this, AFM and a number of custom instruments have been employed thus far [24]–[28]. From these, it is known that collagen fibrils reveal a strongly non-linear stress-response to deformation with the tensile modulus reaching the gigapascal range.

This paper focuses on the control method for the nanomechanical tensile test of the collagen fibril. Most of the conventional nanomanipulation methods have dealt with rigid objects such as metal. On the other hand, the collagen fibril is fragile. Therefore, it is necessary to implement precise force control for this tensile test. However, collagen fibrils typically have a non-linear stress response to deformation, which is causing a modeling error. For precise force control, high responsiveness in the force control and robustness about property change of the collagen fibril are needed.

For high responsiveness in the nanoscale positioning system, a two-degrees-of-freedom (2-DOF) controller has been widely used [29]–[31]. The 2-DOF control is composed of feedforward (FF) and feedback (FB) controllers. FF controller contributes to the rapid motion for this tensile test, and FB controller is used for the disturbance compensation. For robustness about property change, several types of robust control methods have been reported [32]–[34]. The disturbance observer (DOB) is one of the practical and useful methods [33]. In addition, several extended control methods based on DOB have been reported [35]–[37]. In the tensile test, the parameters of the object change, which causes the non-linear material characteristics. This paper also proposes the modeling error compensator (MEC) based on DOB for the parameter change of the load-side in the nanoscale.

This paper proposes the 2-DOF control system with the MEC. To achieve high responsiveness and flexible motion due to the non-linearity of the collagen fibril, the 2-DOF controller is applied to the nanoscale force control. In addition, the MEC is implemented for robustness. The modeling error compensation is calculated from the difference between the actual force response measured by the sensor and the ideal force response calculated from the plant model. By using the proposed method, the nanomechanical tensile test of the collagen fibril was conducted. The validity of the proposed control method was confirmed from the simulation and experimental results.

The contributions of this study are summarized as follows:

- 1) We report the first force-controlled tensile tests of individual collagen fibrils. This will enable direct measurement of viscoelastic material properties of individual collagen fibrils after future development steps.
- 2) To account for non-linear material characteristics, the 2-DOF controller with the MEC is proposed. The proposed method is treated as the nanoscale force controller with high responsiveness and robustness.
- 3) For the confirmation of the above-mentioned contributions, the experimental system is modeled. The validity of the proposed system is experimentally confirmed.

The rest of the paper is organized as follows. Section II explains the nanomechanical system for the tensile test. Section III proposes the 2-DOF controller with the MEC. In addition, the influence of the modeling error is analyzed. Section IV and V show the simulation and experimental results to confirm the validity of the proposed method. Section VI concludes this research.

II. NANOMECHANICAL SYSTEM FOR TENSILE TEST

This section shows the nanomechanical system for the tensile test of the collagen fibril. Fig. 1 shows the nanomechanical system in this research. This nanomechanical system consists of a cantilever with the force sensor, the piezoelectric actuator, and the microscope.

Fig. 2 shows the concept of the tensile test of the collagen fibril. One end of the collagen fibril is placed at the top of the cantilever. The other end of the collagen fibril is fixed

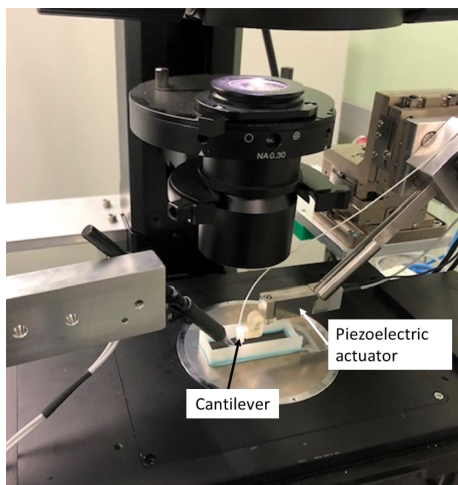


FIGURE 1. Nanomechanical system.

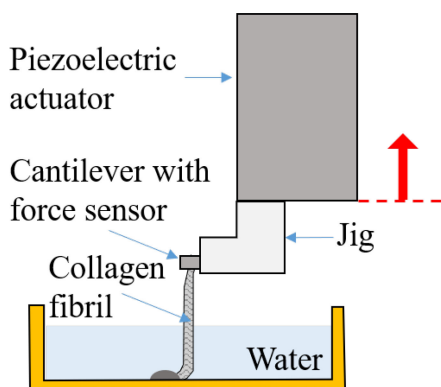


FIGURE 2. Concept of tensile test.

to the water bottom with epoxy. The cantilever is integrated with the piezoelectric actuator through the jig. By moving the piezoelectric actuator upward, the tensile test of the collagen fibril is conducted.

Fig. 3 shows the modeling of the tensile test by the nanomechanical system. In Fig. 3, subscripts \circ_p , \circ_c , and \circ_f mean values related to the piezoelectric actuator, cantilever, and collagen fibril, respectively. x and f represent position and force information. The movement of the piezoelectric actuator is distributed to movements of the cantilever and the collagen fibril.

$$x_p = x_c + x_f \quad (1)$$

The pulling force of the tensile test is calculated from the spring coefficient, and the bending of the cantilever.

$$f_c = K_c x_c \quad (2)$$

where K_c is the spring coefficient of the cantilever. In the experiment, f_c is measured by the force sensor. The equation of motion of the collagen fibril is expressed as follows.

$$M_f \ddot{x}_f + D_f \dot{x}_f + K_f x_f = f_c \quad (3)$$

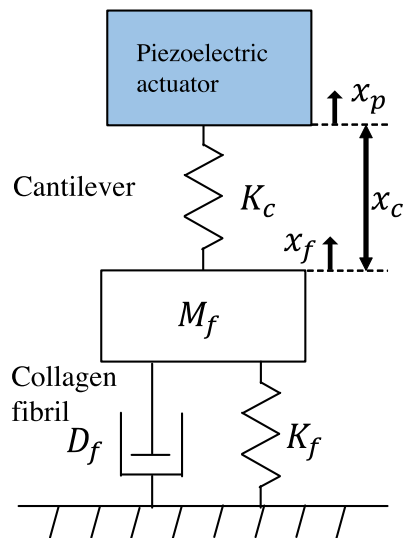


FIGURE 3. Modeling of nanomechanical system.

where M_f , D_f , and K_f represent the mass, damper, spring coefficients of the collagen fibril. Since these values are changed during the tensile test, it is hard to conduct the precise tensile test at the constant force.

To pull the collagen fibril, this paper uses the piezoelectric actuator (P-601, Physik Instrument GmbH & Co. KG.). This piezoelectric actuator has a strain gauge position sensor, and it is possible to implement the closed loop control by using its sensor. From the specification, the linearity error (closed loop) is 0.1 %. Therefore, since the linearity error is small, this piezoelectric actuator is modeled as the linear system.

Fig. 4 shows the Bode plot of this piezoelectric actuator. The input and output of the Bode plot were the input voltage and position response measured by the strain gauge position sensor. Since the linearity error of this piezoelectric actuator is small, there is a linear relationship between the input voltage and the position command. The solid blue line in Fig. 4 shows the frequency response of the sensor voltage. The characteristic is measured using a dynamic signal analyzer (3562 A, Agilent Technologies, Inc.). The dashed red line in Fig. 4 shows the fitting model of the frequency response. Control performances of piezoelectric actuators are typically restricted by system dynamics at low frequencies. Therefore, high-frequency dynamics are not modeled for this first force-controlled tensile test. This enables to keep the order of the model and the designed controller low for control implementation. This model is used for the simulation to confirm the validity of the proposed method.

III. PROPOSED METHOD

This section proposes the control method for the realization of the tensile test of the collagen fibril. Fig. 5 shows the block diagram of the proposed method. The force command generator creates the force command f_c^{cmd} for the tensile test. The proposed control method consists of the 2-DOF controller and the MEC. The 2-DOF controller is composed of

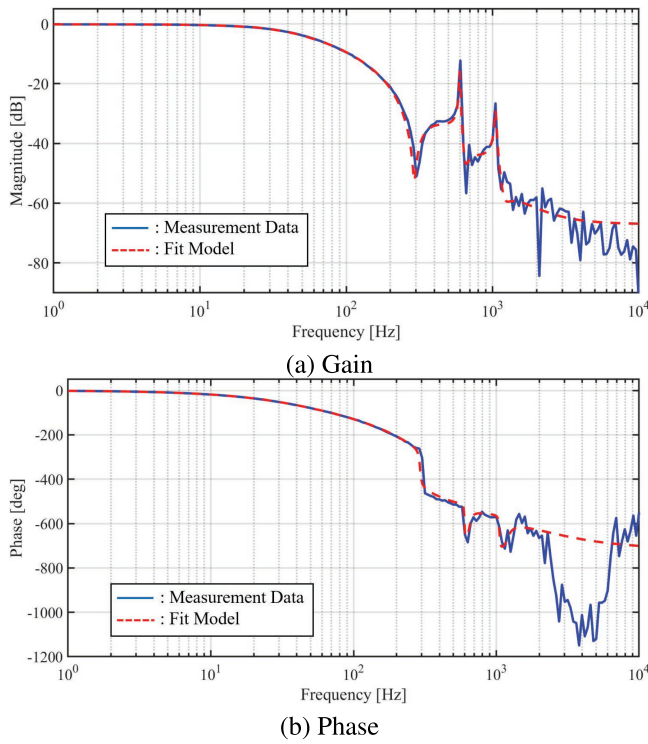


FIGURE 4. Bode plot of piezoelectric actuator.

FF and FB controllers. The modeling error is estimated from the difference between the actual force response measured by the sensor and the ideal force response calculated from the plant model. For the compensation of the modeling error, the estimation value of the modeling error is added to FF input in real-time. By using the proposed control method, the position command of the piezoelectric actuator x_p^{cmd} is calculated. The plant in this system is composed of the piezoelectric actuator, cantilever, and collagen fibril. By the closed loop, the piezoelectric actuator achieves the position command of the piezoelectric actuator x_p^{cmd} . Due to the movement of the piezoelectric actuator, the cantilever pulls the collagen fibril with f_c^{res} as shown in Fig. 2. The position relationship of x_p^{res} , x_c^{res} , and x_f^{res} is expressed as (1). As a result, the tensile test of the collagen fibril is conducted.

The position command of the piezoelectric actuator x_p^{cmd} is expressed as follows.

$$x_p^{cmd} = x_p^{FF} + x_p^{FB} \quad (4)$$

where x_p^{FF} and x_p^{FB} mean the FF and FB position commands of the piezoelectric actuator.

The FF position command is calculated from the force command of cantilever f_c^{cmd} , the modeling error compensation f_c^{cmp} , and the inverse models of the cantilever and collagen fibril.

$$x_p^{FF} = \left(G_c^{nom-1} + G_f^{nom} \right) (f_c^{cmd} + f_c^{cmp}) \quad (5)$$

where G_c and G_f represent the model of the cantilever and collagen fibril ($G_c = K_c$, and $G_f = \frac{1}{M_f s^2 + D_f s + K_f}$). The superscript \circ^{nom} means the value of the nominal model.

In this paper, these nominal models are designed as follows;

$$G_c^{nom} = K_c^{nom} \quad (6)$$

$$G_f^{nom} = \frac{1}{M_f^{nom} s^2 + D_f^{nom} s + K_f^{nom}} \quad (7)$$

where K_c^{nom} and s depict the nominal spring coefficient of the cantilever and Laplace operator. M_f^{nom} , D_f^{nom} , and K_f^{nom} represent the nominal mass, damper, and spring coefficients of the collagen fibril. K_c^{nom} is decided from the cantilever specification.

During the tensile test of collagen fibril, the parameters of the collagen fibril and cantilever are changed in real-time. Due to the change of these parameters, the strongly non-linear stress-response to deformation is revealed. By this phenomenon, the modeling error between the actual plant and the nominal model occurs. In order to compensate for this modeling error, the modeling error compensation f_c^{cmp} is calculated.

$$f_c^{cmp} = \hat{f}_c^{res} - f_c^{res} \quad (8)$$

$$\hat{f}_c^{res} = \frac{G_c^{nom}}{1 + G_c^{nom} G_f^{nom}} x_p^{res} \quad (9)$$

where \hat{f}_c^{res} and x_p^{res} mean the force estimation value of the cantilever and position response of the piezoelectric actuator. $\hat{\circ}$ means the estimated value. \hat{f}_c^{res} is calculated from the nominal model of the cantilever and collagen fibril.

The FB position command is generated by the difference between the force command and response of the cantilever.

$$x_p^{FB} = C_{FB}(f_c^{cmd} - f_c^{res}) \quad (10)$$

where C_{FB} and f_c^{res} mean the feedback controller and the force response of the cantilever. In this paper, PI control is used as the feedback controller ($C_{FB} = K_p + \frac{K_i}{s}$). K_p and K_i are the feedback proportional and integral gains. The force response f_c^{res} is measured by the force sensor.

The performance analysis of the modeling error is shown. Fig. 6 shows the block diagram for the performance analysis. For this analysis, the transfer function from f_c^{cmd} to f_c^{res} is calculated. This paper compares the feedback controller and the 2-DOF controller with/without the MEC.

Fig. 6(a) shows the block diagram of the feedback controller. From Fig. 6(a), the transfer function is calculated.

$$f_c^{res} = \frac{G_{cf} G_p C_{FB}}{1 + G_{cf} G_p C_{FB}} f_c^{cmd} \quad (11)$$

where G_{cf} is the transfer function combining G_c and G_f ($G_{cf} = \frac{G_c}{1 + G_c G_f}$). If it is possible to set high gain in C_{FB} , (11) is rewritten as follows ($G_{cf} G_p C_{FB} \gg 1$).

$$f_c^{res} = \frac{G_{cf} G_p C_{FB}}{1 + G_{cf} G_p C_{FB}} f_c^{cmd} \quad (12)$$

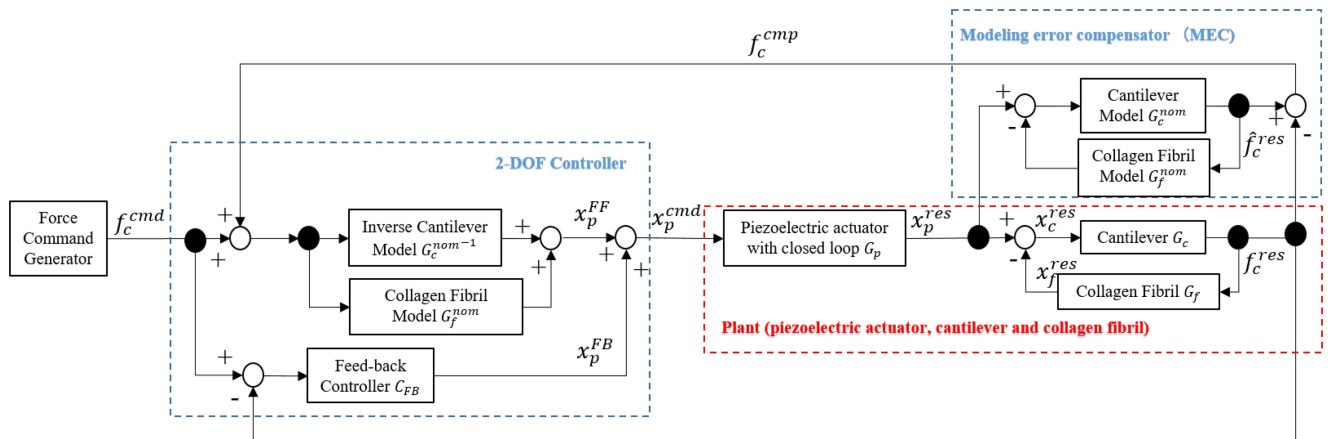


FIGURE 5. Block diagram of proposed method.

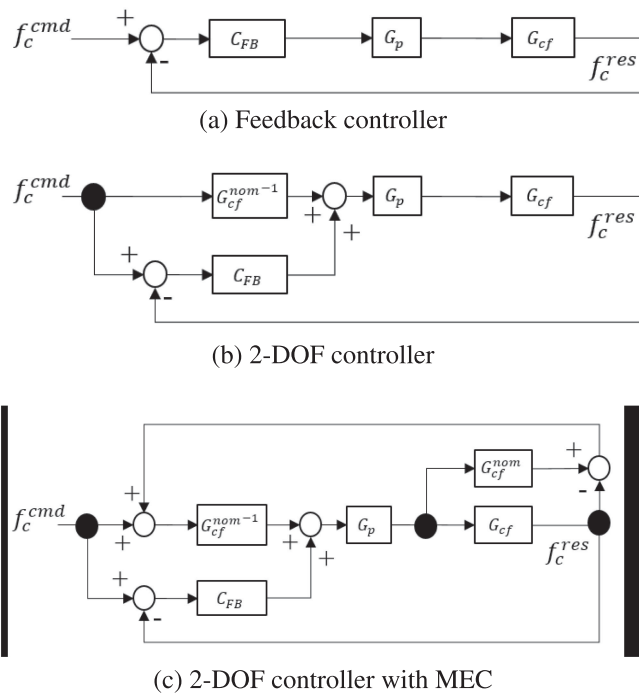


FIGURE 6. Block diagram for performance analysis. (a) Feedback controller (b) 2-DOF controller (c) 2-DOF controller with MEC.

$$\approx f_c^{cmd} \quad (13)$$

However, there is the limitation to setting high gain. Therefore, (13) may not be achieved in most actual cases.

Fig. 6(b) shows the block diagram of the 2-DOF controller without the MEC. From Fig. 6(b), the transfer function is calculated.

$$f_c^{res} = \frac{G_{cf}G_pG_{cf}^{nom-1} + G_{cf}G_pC_{FB}}{1 + G_{cf}G_pC_{FB}} f_c^{cmd} \quad (14)$$

For the pulling test, the piezoelectric actuator worked at low frequencies due to the dynamics of the collagen fibril. As shown in Fig. 4, G_p is assumed as 1 at low frequencies

($G_p \approx 1$). From this assumption, (14) is rewritten as follows.

$$f_c^{res} \approx \frac{G_{cf}G_{cf}^{nom-1} + G_{cf}C_{FB}}{1 + G_{cf}C_{FB}} f_c^{cmd} \quad (15)$$

In (15), G_{cf}^{nom} is not the same as G_{cf} , because of the modeling error ($G_{cf}^{nom} \neq G_{cf}$). Therefore, the force response of the cantilever is not equal to the force command of the cantilever.

Fig. 6(c) shows the block diagram of the 2-DOF controller with the MEC as the proposed method. The transfer function is described as follows.

$$f_c^{res} = \frac{G_{cf}G_pG_{cf}^{nom-1} + G_{cf}G_pC_{FB}}{(1 - G_p) + G_{cf}G_pG_{cf}^{nom-1} + G_{cf}G_pC_{FB}} f_c^{cmd} \quad (16)$$

If $G_p \approx 1$, (16) is rewritten as follows.

$$\begin{aligned} f_c^{res} &\approx \frac{G_{cf}G_{cf}^{nom-1} + G_{cf}C_{FB}}{G_{cf}G_{cf}^{nom-1} + G_{cf}C_{FB}} f_c^{cmd} \quad (17) \\ &= f_c^{cmd} \quad (18) \end{aligned}$$

As shown in (18), the influence of the modeling error to the force response of the cantilever is compensated. As a result, the force command is achieved by the proposed method.

IV. SIMULATION

This section confirms the validity of the proposed method by comparing the proposed and conventional methods in the simulation. For the comparison between the conventional and proposed methods, the FB controller (FB only), the 2-DOF controller (2-DoF w/o MEC), and the 2-DOF controller with the MEC (2-DoF w/ MEC) are implemented. Two types of simulations were conducted.

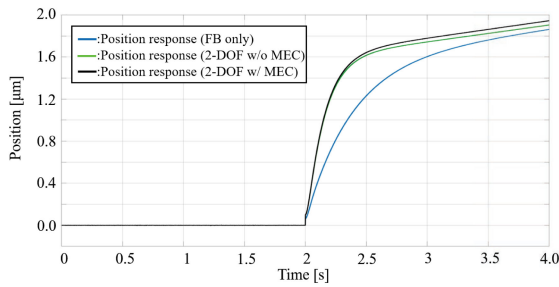
Case 1: There was no modeling error of the nominal model.

Case 2: There was 20 [%] modeling error of the nominal model.

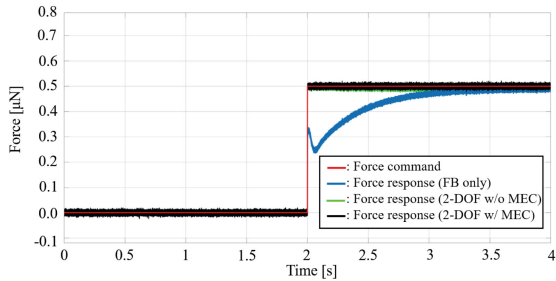
Table 1 shows the parameters of the tensile test. The value of the spring coefficient of the cantilever was set by the specification of the cantilever. The parameters related to the collagen fibril were designed based on the initial

TABLE 1. Parameters of Tensile Test

Parameters	Description	Values
K_c	Spring Coefficient of Cantilever	5.0 [N/m]
K_f	Spring Coefficient of Collagen Fibril	0.33 [N/m]
D_f	Damper Coefficient of Collagen Fibril	0.05 [Ns/m]
M_f	Mass Coefficient of Collagen Fibril	0.01 [g]
K_e	Extension coefficient	0.33 [m/N]
K_p	Feedback Proportional Gain	0.1
K_I	Feedback Integration Gain	4.0
S_t	Sampling Time	0.001 [s]



(a) Position response



(b) Force response

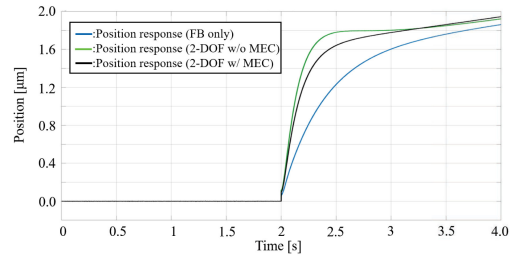
FIGURE 7. Simulation results (Case 1).

state of the actual collagen fibril. The parameters for the FB controller were decided by trial and error. During the tensile test, the parameters of the collagen fibril were changed due to the cantilever force. This parameter change was simulated as the collagen fibril extension. In the simulation, the collagen fibril extension x_f^{ext} was modeled as follows.

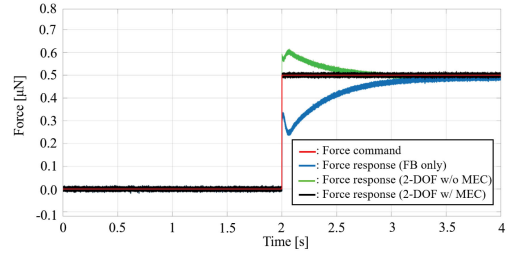
$$x_f^{ext} = K_e \int f_c^{res} dt \quad (19)$$

where K_e means the extension coefficient. This extension was assumed as the plastic deformation. The collagen fibril extension x_f^{ext} was added to x_f^{res} . A step input of 0.5 [μ N] was given as the force command f_c^{cmd} at 2.0 [s].

Figs. 7–8 show the simulation results in Case 1 and Case 2. Figs. 7–8(a) and Figs. 7–8(b) show the position response and force response. Blue, green and black lines represent responses related to the FB only, the 2-DOF w/o MEC, and the 2-DOF w/ MEC. Red line in Figs. 7–8(b) represents the force command. The vibration of the force response is due to the observation noise simulating the accuracy of the force sensor.



(a) Position response



(b) Force response

FIGURE 8. Simulation results (Case 2).

In Case 1, there is no modeling error of the nominal model. As shown in Fig. 7(a), the collagen fibril was extended during the tensile test. This extension value was based on the force response of the cantilever. In Fig. 7(b), the force responses followed the force command. In the FB only as the conventional method, there was the delay of the force response to force command at 2.0 [s]. In both the 2-DOF w/o MEC, and the 2-DOF w/ MEC, the quick responses were achieved at around 2.0 [s]. Therefore, the FF controller contributed to responsiveness, if there is no modeling error.

In Case 2, there was 20 [%] modeling error of the nominal model. As shown in Fig. 8(b), there was the overshoot in the 2-DOF w/o MEC as the conventional method. The reason for this overshoot was the modeling error of the FF controller. In the 2-DOF w/ MEC as the proposed method, this modeling error was compensated by the MEC. Therefore, even if there is the modeling error of the nominal model, the quick response was achieved.

From these simulation results, the validity of the proposed method was confirmed.

V. EXPERIMENT

This section shows the experimental results to confirm the validity of the proposed method. Fig. 1 shows the nanomechanical system in this experiment. This nanomechanical system consists of the cantilever with the force sensor, the piezoelectric actuator, and the microscope. Fig. 9 shows the relationship between the cantilever and the collagen fibril. Fig. 9(a) and (b) show the microscope image and the sketch. For pulling experiments, the collagen fibril by attaching a magnetic bead was prepared. The microgripper was attached to the top of the cantilever. The optical fiber was installed on the cantilever to measure the pulling force (Optics11, Netherlands). By using the magnetic force, the magnetic bead

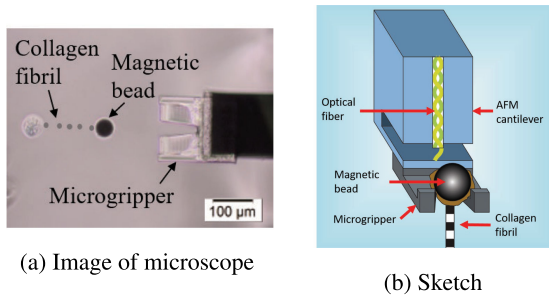


FIGURE 9. Relationship between cantilever and collagen fibril.

was brought to the tip of the microgripper. As shown in Fig. 9, the magnetic bead was pulled by the microgripper attached to the cantilever. The collagen fibril was sourced from the tail tendon of a mouse aged 14 months. The process of isolating individual collagen fibrils from a tendon is described in detail in [38].

The parameters in the experiments were the same as those in the simulation. The parameters of the nominal model in the proposed controller were designed based on the initial state of the collagen fibril. The length of the collagen fibril has an individual difference. Therefore, the initial position (initial input voltage) in each experiment is different. For fair compensation, the steady state with a tensile force of 0.5 [μN] is defined as the initial state in this experiment. A step input of 0.5 [μN] from the initial force value 0.5 [μN] was given as the force command f_c^{cmd} at 2.0[s]. To our best knowledge, this is the first force-controlled tensile test of the collagen fibril. Therefore, the step input was implemented to evaluate the control performance of the force-controlled tensile test. The experimental tendencies for step responses with several amplitudes were almost the same. Therefore, this paper shows the experimental results of the step response with one amplitude. To confirm the validity of the proposed method, three types of controllers were implemented; the FB controller (FB only), the 2-DOF controller without the MEC (2-DoF w/o MEC), and the 2-DOF controller with the MEC (2-DoF w/ MEC).

Fig. 10 shows experimental results. Fig. 10(a), (b) and (c) show the position response, force response and strain. As shown in Fig. 10(a), the collagen fibril was extended due to the pulling force. In Fig. 10(b), force responses with the FB only, 2-DoF w/o MEC, and 2-DoF w/ MEC followed the force command. At 2.0 [s], the step input was given. After the step input, there was the force error between the force command and force response with the FB only. From this fact, responsiveness in the 2-DoF was better than the one in the FB only. Due to the modeling error, the force overshoot in the 2-DoF w/o MEC was larger than one in the 2-DoF w/ MEC. Though there was the overshoot at the moment of adding step input, the force response in the 2-DoF w/ MEC rapidly followed the force command. Table 2 shows the force error between the force command and the force response in the transient state and steady state. Table 3 shows the overshoot and the settling time to evaluate the transient state. As shown

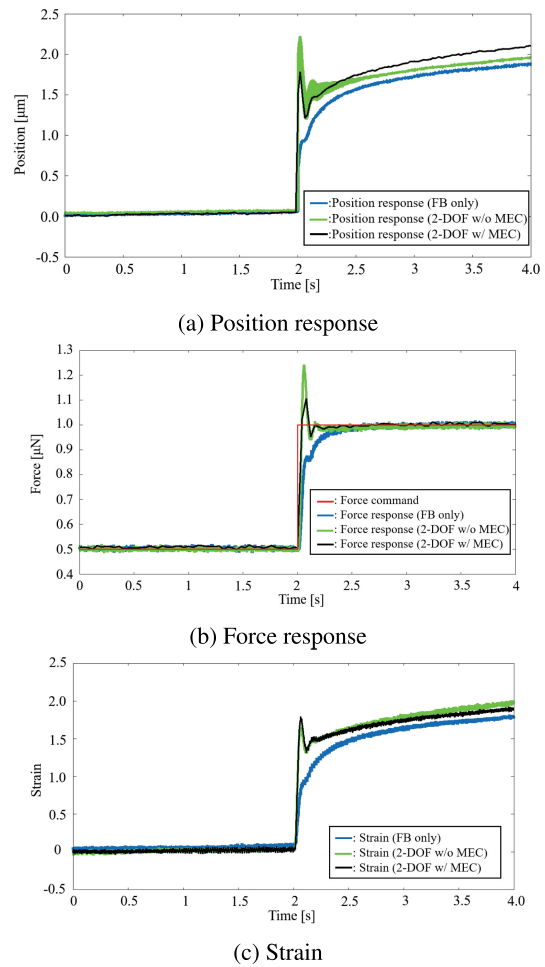


FIGURE 10. Experimental results.

TABLE 2. Force Error (Experimental Results)

(a) Transient State		
	Average [μN]	Variance [μN^2]
FB only	5.0×10^{-2}	6.7×10^{-3}
2-DoF w/o MEC	1.6×10^{-2}	5.1×10^{-3}
2-DoF w/ MEC	9.5×10^{-3}	4.8×10^{-3}
(b) Steady State		
	Average [μN]	Variance [μN^2]
FB only	3.7×10^{-3}	3.0×10^{-5}
2-DoF w/o MEC	3.7×10^{-3}	4.4×10^{-5}
2-DoF w/ MEC	1.0×10^{-3}	4.0×10^{-5}

in Table 2, the average and variance of the force error in the 2-DoF w/ MEC were smaller than those in the conventional methods. As shown in Table 3, though there was overshoot in the 2-DoF w/o MEC and the 2-DoF w/ MEC, the settling time in the 2-DoF w/ MEC was smaller than those in the conventional methods.

The collagen fibril strain can be calculated by measuring the length before tensile testing with the optical microscope. The deformation of the collagen fibril corresponds to the piezo actuator position corrected with the cantilever deflection. Consequently, the deformation can be normalized with

TABLE 3. Overshoot and Settling time(Experimental Results)

	Overshoot [μN]	Settling time [s]
FB only	2.33×10^{-2}	0.408
2-DoF w/o MEC	2.42×10^{-1}	0.369
2-DoF w/ MEC	1.09×10^{-1}	0.296

the initial collagen fibril length. The relative collagen fibril strain in response to the force step is plotted versus time in Fig. 10(c). The force overshoot of the model-based controller only contributes in part to an overshoot in strain mainly due to the viscoelastic nature of collagen fibrils. The apparent stiffness of viscoelastic collagen fibrils is increasing with deformation velocity due to a dashpot contributing to the overall stiffness [39]. Since the model-based controller has a sharper rising edge in both, force and strain signal caused by faster deformation velocity, the apparent stiffness of the collagen fibril yields a less pronounced overshoot in strain. The model-based controller with its faster settling and rise time resembles more closely an idealized step-input that is desired in a creep test of collagen fibrils. Qualitatively, the creep behavior, e.g. strain over time, is similar with both types of controllers while the model-based controller enters a steady-state behavior faster and at higher strains (0.2 %) than the FB only. The choice of controller is a trade-off between overshoot and responsiveness, while the overshoot in collagen fibril strain is not considered as severe when performing a creep experiment. Moreover, the model-based controller is desired when conducting such experiments for the previously discussed reason of more similarity to a force step input compared to the FB only.

From these experimental results, the validity of the proposed method was confirmed from the experimental results.

VI. CONCLUSION

In this paper, we reported the first force-controlled tensile tests of individual collagen fibrils. We proposed a 2-DOF control system with the MEC for force-controlled tensile tests of individual collagen fibrils. Due to the non-linear stress-response to deformation, the modeling error is caused. Therefore, it is necessary to implement precise force control with high responsiveness and robustness. For high responsiveness, the 2-DOF controller was applied to nanoscale force control. For robustness, the modeling error compensation was implemented. Therefore, the proposed method is treated as the nanoscale force controller with high responsiveness and robustness. By using the proposed method, the precise pulling motion for the collagen fibril was achieved. The validity of the proposed control method was confirmed from the simulation and experimental results.

The future works of this research are described as follows:

- 1) With the presented work, the creep behavior of collagen fibrils can be measured. This will allow for studying the effects of diseases and aging on connective tissues. In a future development step, a sinusoidal force will be used to conduct dynamic mechanical analysis on individual

collagen fibrils. Other fibers at the micro and nanoscale such as electrospun polymer fibers will be investigated as well.

- 2) For further performance improvement, the control method will be improved to suppress the overshoot. In addition, the stability and sensitivity characteristics are also important. We will analyze the stability and sensitivity characteristics.
- 3) From the viewpoint of biomechanics, the specification of the force-controlled tensile tests will be clarified.

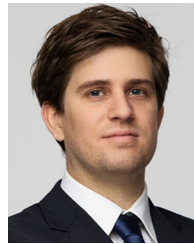
REFERENCES

- [1] T. Atsumi and S. Yabui, "Quadruple-stage actuator system for magnetic-head positioning system in hard disk drives," *IEEE Trans. Ind. Electron.*, vol. 67, no. 11, pp. 9184–9194, Nov. 2020.
- [2] S. Xiong and D. B. Boggy, "Hard disk drive servo system based on field-programmable gate arrays," *IEEE Trans. Ind. Electron.*, vol. 61, no. 9, pp. 4878–4884, Sep. 2014.
- [3] M. F. Heertjes, "Variable gain motion control of wafer scanners," *IEEJ J. Ind. Appl.*, vol. 5, no. 2, pp. 90–100, 2016.
- [4] K. Ohno, K. Ito, T. Yamada, J. Sato, Y. Shiroyama, and T. Hamajima, "Disturbance suppression considering thrust constant fluctuation and restoring force of flat cable for precise force control," *IEEE Trans. Ind. Electron.*, vol. 68, no. 1, pp. 882–891, Jan. 2021.
- [5] W. Gao *et al.*, "Precise automated intracellular delivery using a robotic cell microscope system with three-dimensional image reconstruction information," *IEEE/ASME Trans. Mechatronics*, vol. 25, no. 6, pp. 2870–2881, Dec. 2020.
- [6] D. Xing, F. Liu, S. Liu, and D. Xu, "Motion control for cylindrical objects in microscope's view using a projection Method-II: Collision avoidance with reduced dimensional guidance," *IEEE Trans. Ind. Electron.*, vol. 64, no. 7, pp. 5534–5544, Jul. 2017.
- [7] T. Tuma, A. Sebastian, J. Lygeros, and A. Pantazi, "The four pillars of nanopositioning for scanning probe microscopy: The position sensor, the scanning device, the feedback controller, and the reference trajectory," *IEEE Control Syst. Mag.*, vol. 33, no. 6, pp. 68–85, Dec. 2013.
- [8] A. J. Fleming, S. S. Aphale, and S. O. R. Moheimani, "A new method for robust damping and tracking control of scanning probe microscope positioning stages," *IEEE Trans. Nanotechnol.*, vol. 9, no. 4, pp. 438–448, Jul. 2010.
- [9] S. Ito, M. Poik, J. Schlarp, and G. Schitter, "Atomic force microscopy breaking through the vertical range-bandwidth tradeoff," *IEEE Trans. Ind. Electron.*, vol. 68, no. 1, pp. 786–795, Jan. 2021.
- [10] M. R. P. Ragazzon, J. T. Gravdahl, and K. Y. Perrersen, "Model-based identification of nanomechanical properties in atomic force microscopy: Theory and experiments," *IEEE Trans. Control Syst. Technol.*, vol. 27, no. 5, pp. 2045–2057, Sep. 2019.
- [11] K. Seki, D. Noda, and M. Iwasaki, "Dual-loop controller design considering robust vibration suppression in piezo-actuated stage systems," *IEEJ J. Ind. Appl.*, vol. 7, no. 6, pp. 488–494, 2018.
- [12] M. L. Nguyen and X. Chen, "MPC inspired dynamical output feedback and adaptive feedforward control applied to piezo-actuated positioning systems," *IEEE Trans. Ind. Electron.*, vol. 67, no. 5, pp. 3921–3931, May 2020.
- [13] J. Chen, G. Peng, H. Hu, and J. Ning, "Dynamic hysteresis model and control methodology for force output using piezoelectric actuator driving," *IEEE Access*, vol. 8, pp. 205136–205147, 2020.
- [14] Y. Shen *et al.*, "Single cell stiffness measurement at various humidity conditions by nanomanipulation of a nano-needle," *Nanotechnol.*, vol. 24, no. 14, pp. 1–9, 2013.
- [15] X. Yang, L. Zhu, S. Li, W. Zhu, and C. Ji, "Development of a novel pile-up structure based nanopositioning mechanism driven by piezoelectric actuator," *IEEE/ASME Trans. Mechatronics*, vol. 25, no. 2, pp. 502–512, Apr. 2020.
- [16] S. Mekid, "Integrated nanomanipulator with in-process lithography inspection," *IEEE Access*, vol. 8, pp. 95378–95389, 2020.
- [17] S. Yuan, Z. Wang, N. Xi, Y. Wang, and L. Liu, "AFM tip position control in situ for effective nanomanipulation," *IEEE/ASME Trans. Mechatronics*, vol. 23, no. 6, pp. 2825–2836, Dec. 2018.

- [18] M. D. Shoulders and R. T. Raines, "Collagen structure and stability," *Annu. Rev. Biochem.*, vol. 78, pp. 929–958, 2009.
- [19] J. A. Petruska and A. J. Hodge, "A subunit model for the tropocollagen macromolecule," *Biochemistry: Petruska Hodge*, vol. 51, pp. 871–876, 1964.
- [20] O. Chaudhuri, J. Cooper-White, P. A. Janmey, D. J. Mooney, and V. B. Shenoy, "Effects of extracellular matrix viscoelasticity on cellular behaviour," *Nature*, vol. 584, pp. 535–546, 2020.
- [21] O. G. Andriotis *et al.*, "Structure-mechanics relationships of collagen fibrils in the osteogenesis imperfecta mouse model," *J. Roy. Soc. Interface*, vol. 12, no. 111, pp. 1–12, 2015.
- [22] J. G. Snedeker and A. Gautieri, "The role of collagen crosslinks in ageing and diabetes—the good, the bad, and the ugly," *Muscles, Ligaments Tendons J.*, vol. 4, no. 3, pp. 303–308, 2014.
- [23] A. Gautieri *et al.*, "Advanced glycation end-products: Mechanics of aged collagen from molecule to tissue," *Matrix Biol.*, vol. 59, pp. 95–108, 2017.
- [24] R. B. Svensson, S. T. Smith, P. J. Moyer, and S. P. Magnusson, "Effects of maturation and advanced glycation on tensile mechanics of collagen fibrils from rat tail and achilles tendons," *Acta Biomaterialia*, vol. 70, pp. 270–280, 2018.
- [25] R. B. Svensson, H. Mulder, V. Kovanen, and S. P. Magnusson, "Fracture mechanics of collagen fibrils: Influence of natural cross-links," *Biophysical J.*, vol. 104, no. 11, pp. 2476–2484, 2013.
- [26] R. B. Svensson, T. Hassenkam, P. Hansen, S. Peter Magnusson, and J. Mech, "Tensile properties of human collagen fibrils and fascicles are insensitive to environmental salts," *Biophysical J.*, vol. 99, no. 12, pp. 4020–4027, 2010.
- [27] Y. Liu, R. Ballarini, and S. J. Eppell, "Tension tests on mammalian collagen fibrils," *Interface Focus*, vol. 6, no. 1, pp. 1–7, 2016.
- [28] Z. L. Shen, M. R. Dodge, H. Kahn, R. Ballarini, and S. J. Eppell, "Stress-strain experiments on individual collagen fibrils," *Biophysical J.*, vol. 95, pp. 3956–3963, 2008.
- [29] I. Ahmad, "Two degree-of-freedom robust digital controller design with bouc-wen hysteresis compensator for piezoelectric positioning stage," *IEEE Access*, vol. 6, pp. 17275–17283, 2018.
- [30] M. L. Nguyen and X. Chen, "MPC inspired dynamical output feedback and adaptive feedforward control applied to piezo-actuated positioning systems," *IEEE Trans. Ind. Electron.*, vol. 67, no. 5, pp. 3921–3931, May 2020.
- [31] S. Hara, T. Hara, L. Yi, and M. Tomizuka, "Novel reference signal generation for two-degree-of-freedom controllers for hard disk drives," *IEEE/ASME Trans. Mechatronics*, vol. 5, no. 1, pp. 73–78, Mar. 2000.
- [32] E. Ostertag, "An improved path-following method for mixed H_2/H_∞ controller design," *IEEE Trans. Autom. Control*, vol. 53, no. 8, pp. 1967–1971, Jul. 2008.
- [33] K. Ohnishi, M. Shibata, and T. Murakami, "Motion control for advanced mechatronics," *IEEE/ASME Trans. Mechatronics*, vol. 1, no. 1, pp. 56–67, Mar. 1996.
- [34] R. Xu, X. Zhang, H. Guo, and M. Zhou, "Sliding mode tracking control with perturbation estimation for hysteresis nonlinearity of piezo-actuated stages," *IEEE Access*, vol. 6, pp. 30617–30629, 2018.
- [35] Y. Yokokura and K. Ohishi, "Fine load-side acceleration control based on torsion torque sensing of two-inertia system," *IEEE Trans. Ind. Electron.*, vol. 67, no. 1, pp. 768–777, Jan. 2020.
- [36] E. Sariyildiz and K. Ohnishi, "An adaptive reaction force observer design," *IEEE/ASME Trans. Mechatronics*, vol. 20, no. 2, pp. 750–760, Apr. 2015.
- [37] T. Yamanaka, K. Yamada, R. Hotchi, and R. Kubo, "Simultaneous time-delay and data-loss compensation for networked control systems with energy-efficient network interfaces," *IEEE Access*, vol. 8, pp. 110082–110092, 2020.
- [38] O. G. Andriotis *et al.*, "Nanomechanical assessment of human and murine collagen fibrils via atomic force microscopy cantilever-based nanoindentation," *J. Mech. Behav. Biomed. Mater.*, vol. 39, pp. 9–26, 2014.
- [39] R. B. Svensson, T. Hassenkam, P. Hansen, and S. P. Magnusson, "Viscoelastic behavior of discrete human collagen fibrils," *J. Mech. Behav. Biomed. Mater.*, vol. 3, no. 1, pp. 112–115, 2010.



2020, he also held the position of a Visiting Professor with Automation and Control Institute, TU Wien, Austria. His research interests include robotics, motion control, and haptics.



lagenous tissues, nanolithography, mechanobiology, and tissue engineering.



high-precision mechatronic systems for production, inspection, and automation, such as vibration isolators, AFMs, laser scanners, and 3D printers.



strumentation for micro and nanomechanical characterization of biological tissues and biomaterials. Dr. Thurner was the recipient of the IFAC Mechatronics Best Paper Award (during 2008–2011).



tech industry, scientific instrumentation, and mechatronic imaging systems, such as AFM, scanning laser and LIDAR systems, telescope systems, adaptive optics, and lithography systems for semiconductor industry.

Dr. Schitter was the recipient of the IFAC Mechatronics Best Paper Award (during 2008–2011) and 2013 IFAC Mechatronics Young Researcher Award, and was an Associate Editor for the IFAC Mechatronics, *Control Engineering Practice*, and IEEE TRANSACTIONS ON MECHATRONICS.

NAOKI MOTOI (Member, IEEE) received the B.E. degree in system design engineering and the M.E. and Ph.D. degrees in integrated design engineering from Keio University, Tokyo, Japan, in 2005, 2007 and 2010, respectively. In 2007, he joined the Partner Robot Division, Toyota Motor Corporation, Japan. From 2011 to 2013, he was a Research Associate with Yokohama National University, Yokohama, Japan. Since 2014, he has been with Kobe University, Kobe, Japan, where he is a currently an Associate Professor. From 2019 to

MATHIS NALBACH received the B.Sc. degree in mechanical and process engineering from TU Darmstadt, Darmstadt, Germany, in 2014, and the M.Sc. degree in biomedical engineering in 2016 from TU Wien, Vienna, Austria, where he is currently working toward the Ph.D. degree with the ILSB, TU Wien, Austria in the topic Development of a Tensile Testing Device for Individual Collagen Fibrils and other Nanofibres. His research interests include AFM based nano and microindentation of soft samples, biomechanics with a focus on collagenous tissues, nanolithography, mechanobiology, and tissue engineering.

SHINGO ITO received the M.A.Sc. degree in mechanical and industrial engineering from the University of Toronto, Toronto, ON, Canada, in 2007 and the Ph.D. degree in electrical engineering from TU Wien, Vienna, Austria in 2015. He was an Engineer with Yaskawa Electric Corporation, Japan, from 2007 to 2010 and as a Researcher with Automation and Control Institute, TU Wien, from 2011 to 2021. He is currently an Associate Professor with the University of Fukui, Fukui, Japan. His research interests include design and control of

PHILIPP J. THURNER received the M.Sc. degree in technical physics from TU Graz, Graz, Austria in 1999, and the Ph.D. degree in natural sciences from ETH Zurich, Zurich, Switzerland, in 2004. He is currently a Professor of Biomechanics with the Institute of Lightweight Design and Structural Biomechanics, TU Wien, Vienna, Austria. His research interests include micro and nanomechanics of both hard and soft collagen-rich tissues and individual collagen fibrils, noncollagenous proteins, bone fracture risk and osteoporosis as well as instrumentation for micro and nanomechanical characterization of biological tissues and biomaterials. Dr. Thurner was the recipient of the IFAC Mechatronics Best Paper Award (during 2008–2011).

GEORG SCHITTER (Senior Member, IEEE) received the M.Sc. degree in electrical engineering from TU Graz, Graz, Austria, in 2000, and the M.Sc. degree in information technology and the Ph.D. degree in technical sciences from ETH Zurich, Zurich, Switzerland, in 2004.